

Ayache Bouakaz, Aya Zeghimi,
and Alexander A. Doinikov

Abstract

Contrast agents for ultrasound are now routinely used for diagnosis and imaging. In recent years, new promising possibilities for targeted drug delivery have been proposed that can be realized by using the microbubble composing ultrasound contrast agents (UCAs). The microbubbles can carry drugs and selectively adhere to specific sites in the human body. This capability, in combination with the effect known as sonoporation, provides great possibilities for localized drug delivery. Sonoporation is a process in which ultrasonically activated UCAs, pulsating nearby biological barriers (cell membrane or endothelial layer), increase their permeability and thereby enhance the extravasation of external substances. In this way drugs and genes can be delivered inside individual cells without serious consequences for the cell viability. Sonoporation has been validated both *in-vitro* using cell cultures and *in-vivo* in preclinical studies. However, today, the mechanisms by which molecules cross the biological barriers remain unrevealed despite a number of proposed theories. This chapter will provide a survey of the current studies on various hypotheses regarding the routes by which drugs are incorporated into cells or across the endothelial layer and possible associated microbubble acoustic phenomena.

Keywords

Sonoporation • Ultrasound • Microbubble • Mechanisms

10.1 Introduction

Targeted drug delivery is one of the most important goals of modern pharmacology and therapy. The strict localization of the pharmacological activity of a drug to the site of action would result in a significant reduction in drug toxicity,

A. Bouakaz (✉) • A. Zeghimi • A.A. Doinikov
Inserm Imaging and Ultrasound,
INSERM U930, Imagerie et Cerveau,
Université François-Rabelais de Tours, Tours, France
e-mail: ayache.bouakaz@univ-tours.fr

reduction of the drug dose, and increased treatment efficacy. Currently a great amount of work is concentrated worldwide on the research of various targeted drug delivery systems. However, this goal still remains unachievable.

In recent years, new promising possibilities for targeted drug and gene delivery have been discovered that can be realized by using ultrasound contrast agents (UCAs). Ultrasound contrast agents are micron-sized encapsulated gas bubbles, which are produced by pharmaceutical companies for medical ultrasound applications (Goldberg et al. 2001; Szabo 2004). The encapsulation is necessary to prevent the microbubbles from fast dissolution in blood and from coalescence. Currently, contrast agents are used in ultrasonic diagnostics. In this case, they are injected into the bloodstream of the patient in order to increase the contrast between blood (microcirculation) and tissue during an ultrasonic examination and thereby to improve the quality of ultrasonic images and diagnosis confidence. Recently, specific contrast agents have been designed, which are capable of selectively adhering to desired target sites in the human body (Bloch et al. 2004; Klivanov 2006). Adhering to specific sites or tissues, such targeted agents can enhance the acoustic differences between normal and abnormal parts of organs and thereby improve the detectability of abnormalities, such as lesions, inflammatory processes and thrombi. Moreover, targeted contrast agents can carry drugs or genes on the encapsulating shell. This capability, in combination with the phenomenon known as sonoporation, provides unprecedented possibilities for a highly selective therapeutic action. The term sonoporation denotes a process in which ultrasonically activated contrast microbubbles, pulsating nearby cells or biological barriers, increase their permeability and thereby enhance the penetration and the extravasation of external substances (Ferrara et al. 2007; Kaddur et al. 2007). This leads to an increase in vascular permeability, thus facilitating the extravasation of drugs into targeted tissue and hence an augmented drug bioavailability without serious consequences for the cell viability (Fig. 10.1). In addition, this delivery system promises to be a

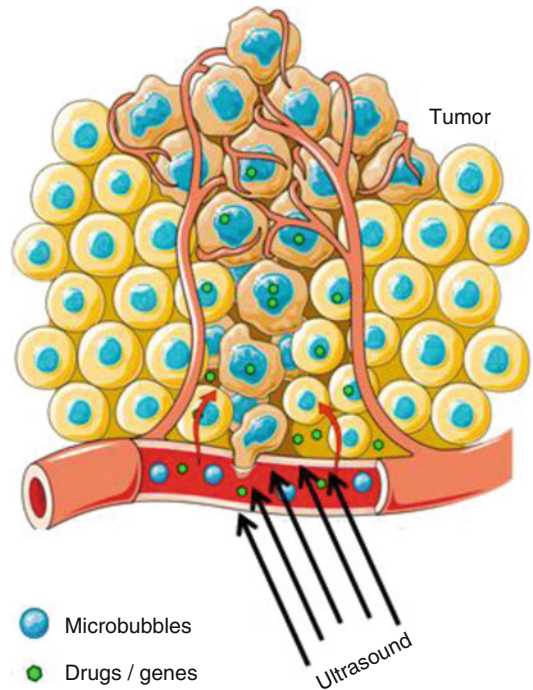


Fig. 10.1 Pictographic essay of sonoporation for drug and gene delivery (Adapted from Servier Medical Art, www.servier.fr)

low-cost technology, which is a notable feature of all ultrasound technologies.

The first experiments on sonoporation date back to the 1980s, where various ultrasound (US) exposure conditions were tested blindly at frequencies ranging from the kHz to the MHz (Ferrara et al. 2007; Escoffre et al. 2013). Sonoporation has also been evaluated using high-pressure amplitude US waves. Since then and with the recent introduction of contrast agents, higher frequency US in conjunction with cavitation has been called on to induce a range of effects on cells. Extensive examinations have been carried out to evaluate the efficiency of US in combination with contrast microbubbles for inducing cellular uptake. Although these results and findings were achieved in a controlled *in-vitro* environment, diagnostic US scanners were also useful for therapeutic applications of sonoporation, particularly with the guidance of treatment afforded by the imaging mode.

One of the first papers that described the use of sonoporation with ultrasound and UCAs dates back to 1997 (Bao et al. 1997). Since then, several studies have been reported on this topic, but so far the exact mechanism of sonoporation responsible for permeabilization remains unrevealed. Available hypotheses suggest that acoustic phenomena, such as stable and inertial cavitation, microstreaming, microjets, and shock waves are involved in the observed permeabilization sequences. All these acoustic phenomena are induced by the oscillations or destructions of microbubbles activated by US waves. Although the results obtained from these studies demonstrate the potential of sonoporation as a therapeutic strategy, they still provide conflicting conclusions. Some studies show that inertial cavitation is required for the induction of drug uptake; whilst others show that stable cavitation is sufficient. Microbubble jetting has been observed near a cell layer, but its effect on drug uptake was not really studied. The influence of microstreaming has rarely been studied in experiments using encapsulated contrast microbubbles, but there are various theoretical approaches. Other studies show that standing waves are required for drug uptake. A few recent reports have shown that oscillating microbubbles can deform cells, which could be a trigger for drug uptake. This suggests that drug uptake can be induced by several acoustic mechanisms. It has been reported that the conclusions about the mechanisms of cell membrane permeabilization are not straightforward despite numerous papers using various cell line models, ultrasound systems and experimental environments. Current investigations report only on drug uptake, electron microscopy observations, or cell electrophysiological measurements but do not address the relationship between microbubble acoustic behavior and drug uptake.

In this chapter, firstly we will present various acoustic phenomena that originate from the interaction of ultrasound waves and microbubbles and that are likely to be involved in the permeabilization of the cell membrane. In the second part, various assumed mechanisms by which molecules or drugs extravasate through the cell

membrane and enter into the cytoplasm after sonoporation will be discussed. Finally, we will give a number of examples of *in-vivo* applications of sonoporation.

10.2 Mechanisms of Barrier Permeabilization and Molecular Delivery

Sonoporation was first demonstrated in the late 80s where kHz frequency ultrasound was evaluated for molecular uptake. This finding was original, although the efficiency of this approach was not fully proved. Following the introduction of ultrasound contrast agents in the late 90s, microbubbles were thought to be associated with a higher molecular uptake. Indeed, microbubbles, which are known to be a pure intravascular tracer, do not cross the endothelial barrier. However, their oscillations next to the endothelial layer might induce the permeabilization of the vessel wall. At the cellular level, microbubble oscillations increase the cell membrane permeability transiently. The availability of different contrasts and various protocols led to a large diversity of results on molecular uptake and efficiency rendering the comparison between them nearly impossible. It is believed that contrast microbubbles can be used as a nuclei trigger to enhance the delivery of drugs and molecules through the biological barriers. Nevertheless, the diversity of the insonation parameters did not allow providing precise conclusions and comparisons between various experimental conditions.

Although the sonoporation efficiency in permeabilizing the cell membrane was demonstrated, mechanisms behind the action of ultrasound and microbubbles were not clearly identified. Therefore several groups were engaged in elucidating the mechanisms responsible for cell membrane permeabilization caused by ultrasound and microbubble insonation. Current investigations report only on drug uptake, electron microscopy observations, or cell electrophysiological measurements but do not address the relationship between microbubble acoustic behavior and drug uptake.

10.2.1 Acoustical Phenomena

Various microbubble acoustic phenomena have been explored and studied to determine their involvement in the sonoporation mechanisms. Microstreaming, microjets, stable and inertial cavitations have been proposed as possible candidates in the transient or permanent permeabilization of the cell membrane. All these acoustic phenomena are induced by the oscillations or destructions of microbubbles activated by US waves.

One of acoustic phenomena that might impact mechanically on the cell membrane to make it permeable is acoustic microstreaming. When a bubble is driven acoustically, it is known to generate steady vortical flows in the surrounding liquid. It has been suggested that this phenomenon, called acoustic microstreaming, plays an important role in various biological effects of ultrasound, such as hemolysis, sonothrombolysis and sonoporation. Early experimental investigations into this phenomenon go back to the work of Kolb and Nyborg (1956) and Elder (1959), where the dependence of acoustic microstreaming on certain parameters (*e.g.*, amplitude of sound) was determined and observations of microstreaming patterns for various amplitudes and viscosities were made. Hughes and Nyborg (1962) were the first to show that bubble-induced vortex streaming can be used for disruption of cells in suspension. Pritchard et al. (1966) established that the number of breaks occurring in DNA molecules was directly related to velocity gradients of acoustic microstreaming. These effects were attributed to shear stresses exerted on cells and large molecules by the microstreaming. Further insights into this mechanism were given by experiments of Rooney (1970, 1972) on hemolysis produced by a single air bubble in an erythrocyte suspension.

The progress of experimental studies on microstreaming can be traced in works by Nyborg (1978), Liu et al. (2002), Tho et al. (2007), Wu and Nyborg (2008), Collis et al. (2010) and Wang et al. (2012). Wu et al. (2002) used a Mason horn with a 0.4 mm probe tip vibrating at 21.4 kHz. The transverse displacement amplitudes were

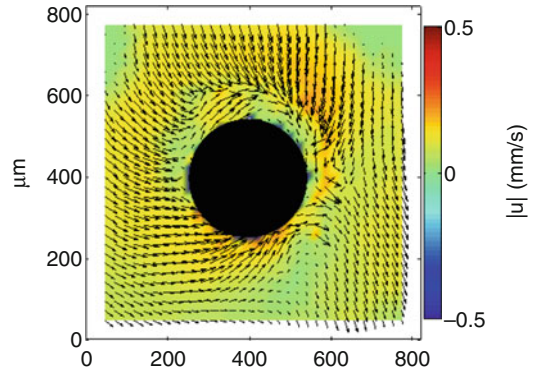


Fig. 10.2 Acoustic microstreaming around an air bubble as recorded with PIV using ultrasound at 28 kHz and 7 kPa

greater than 7.8 μm and produced shear stresses on the Jurkat cell suspension due to microstreaming. The authors believe that the generated microstreaming around the probe tip was the main reason for the cell reparable sonoporation, inducing the uptake of fluorescent dextran molecules. The threshold was estimated to be 12 Pa for an exposure time of up to 7 min (Ross et al. 2002).

Shear stresses generated by relatively large bubbles have been recorded using a particle imaging velocity (PIV) system. The PIV measurements were performed for bubbles of different sizes ranging from 200 to 400 μm (Novell et al. 2011). The results showed that the flow velocity exhibited a first peak near the bubble resonance. For this bubble, the shear stress is also maximal. The experimental measurements also revealed a second peak for bubbles larger than the resonance size but with lower amplitude. Figure 10.2 demonstrates an example of PIV images showing the microstreaming generated around a bubble of 200 μm in diameter at 28 kHz and an acoustic pressure of 7 kPa.

First theoretical studies on bubble-induced microstreaming were performed by Nyborg (1958). In particular, his theory gives a formula for shear stresses exerted on a rigid plane by a pulsating hemispherical bubble resting on this plane. This formula was used by Rooney (1972) for estimating shear stresses experienced by cells near a pulsating bubble. To apply Nyborg's formula to nonlinear bubble oscillations, Lewin and Bjørnø (1982) suggested combining

Nyborg's formula with the Rayleigh-Plesset equation. The combination of Nyborg's formula with the de Jong shell model was used by Wu (2002) to estimate shear stresses generated by contrast agent microbubbles. It was pointed out by Doinikov and Bouakaz (2010c) that the use of Nyborg's formula, which was derived for a hemispherical bubble, is not correct in the case of an encapsulated bubble. To solve this problem, they recalculated Nyborg's formula for the case of a spherical bubble being at a distance from a rigid plane. The same result, in a simplified formulation, was obtained by Yu and Chen (2014). Numerical simulations of shear stresses produced by free and encapsulated bubbles on a rigid wall were performed by Krasovitski and Kimmel (2004) using the boundary integral method. They came to the conclusion that the bubble-induced stress is several orders of magnitude greater than the physiological stress induced on the vessel wall by the flowing blood.

There are a number of theoretical models for the velocity and stress fields of acoustic microstreaming that is developed around a bubble in an unbounded liquid. Davidson and Riley (1971) derived equations for microstreaming generated by a bubble undergoing translational harmonic oscillations. Wu and Du (1997) and Longuet-Higgins (1998) considered the case of a bubble undergoing translational and radial oscillations. Maksimov (2007) extended the result of Longuet-Higgins (1998) so as to include the effect of parametrically excited surface modes of high order. Liu and Wu (2009) applied the approach of Wu and Du (1997) to calculate microstreaming produced by an encapsulated bubble. Doinikov and Bouakaz (2010a, b) extended the results of Wu and Du (1997) and Liu and Wu (2009) by taking into account shape oscillations and removing restrictions such as the assumption that the thickness of the viscous boundary layer surrounding the bubble is much smaller than the radius of the bubble. Doinikov and Bouakaz (2010b) also derived equations for acoustic microstreaming generated by a bubble in the presence of a distant rigid wall. They showed that the presence of the wall can change the amplitude and the phase of the bubble oscillations in such a way that the

intensity of acoustic microstreaming is increased considerably as compared to that generated by the same bubble in an infinite liquid.

The shear mechanism has also been investigated optically. The interaction of an oscillating microbubble with cells has been observed with a high-speed camera (van Wamel et al. 2004). The observations with the use of endothelial cells revealed a strong mechanical action of SonoVue microbubbles insonified with a single ultrasound burst at 1 MHz and 0.9 MPa acoustic pressure. This action induces oscillatory stresses that pull and push the cell membrane, termed here cellular massage, and likely trigger various cellular and intracellular responses.

Besides microstreaming and shear stresses, other acoustic phenomena related to microbubble oscillations have been regarded as possibly responsible for or involved in the sonoporation mechanisms and effective in permeabilizing the cell membrane at megahertz frequencies and at acoustic pressures as low as a few MPa. Shock waves and liquid microjets generated in the course of inertial cavitation are among such phenomena.

Although the dominant hypothesis is now that sonoporation is caused by shear stresses exerted on the cell membrane by acoustic microstreaming, there are suggestions that pressure shock waves and liquid microjets generated by cavitating bubbles make a contribution as well. Interest in the above phenomena goes back to applied hydrodynamic problems such as cavitation damage of ship propellers and hydraulic turbine blades and ultrasonic cleaning of contaminated surfaces. The literature on the subject is very extensive. There are a number of reviews, written in different years, that describe at length available experimental observations: Plesset and Prosperetti (1977), Mørch (1979), Blake and Gibson (1987), Leighton (1994), Brennen (1995) and Lauterborn and Kurz (2010). Experimental estimates show that the spherical shock wave produced by a collapsing bubble may have an amplitude of up to 1 GPa but this shock so rapidly dies down that its impact may be significant only at distances of about the initial bubble radius. However, in a concentrated bubble cluster, the combined shocks from many collapsing bubbles

can cause damage at much greater distances. The feasibility of this process was supported by the experimental observations of Brunton (1967), Vyas and Preece (1976) and Shima et al. (1983).

A hypothesis that the asymmetric collapse of a bubble might generate a liquid microjet was first put forward by Kornfeld and Suvorov (1944). The first experimental and theoretical evidence of this phenomenon was provided by Naudé and Ellis (1961) and later Benjamin and Ellis (1966). Modern experimental techniques reached the stage where collapsing bubbles can be filmed at framing rates of up to 100 million frames per second: see Lauterborn (1972), Vogel et al. (1989), Field (1991), Ohl et al. (1999) and Lindau and Lauterborn (2003). Particularly impressive experiments were performed by Lindau and Lauterborn (2003). They observed the bubble jetting and shock wave emissions using high-speed cinematography of laser-produced cavitation bubbles near a rigid boundary. Experiments in which the effect of a compliant elastic boundary on the bubble collapse is investigated are reported by Brujan et al. (2001a, b). In particular, Brujan et al. observed that the interaction of a collapsing bubble with a boundary consisting of a polyacrylamide gel with 80 % water concentration could lead to, depending on conditions, bubble splitting, formation of liquid jets away from and towards the boundary, and jet-like ejection of the boundary material into the surrounding liquid.

Much work has been done on numerical modeling of bubble collapse and jet formation. Most numerical studies are based on various modifications of the boundary integral method and focus on modeling the aspherical collapse of a bubble near a rigid boundary with the formation of a liquid jet. Comparisons of measured and simulated results, for example, those made by Lauterborn and Bolle (1972) for the bubble shape at the initial stages of the collapse and Vogel et al. (1989) for liquid flow velocities during the jetting process, demonstrate good agreement.

Biomedical applications have given new impetus to studies on shock waves and microjets generated by cavitating bubbles. Kudo et al. (2009) reported that the generation of liquid microjets caused cell membrane perforation.

Similar results were reported previously by Ohl et al. (2006). They investigated experimentally the interaction of a cell monolayer in the culture dish with ultrasound at high peak negative acoustic pressures (4 MPa) and observed that the high intensity ultrasound caused the detachment of cells at the focal depth. Using optical observations, they observed cell removal and showed the cells at the edge of the area became permanently porated and the surrounding cells incorporated the fluorescent marker, calcein. These observations were associated with the collapse of large cavities, which generated a strong fluid flow field. In a separate study, these cavities were assumed to be of the order of tens of micrometers as described by Le Gac et al. (2007).

Koshiyama et al. (2006, 2008) conducted a series of full atomistic molecular dynamics simulations of cell membrane models (lipid bilayers) subject to shock waves. They observed that shock impulses caused the compression and the rebound of the lipid bilayer in the course of which water molecules penetrated inside the hydrophobic core of the membrane. However, in none of these simulations, the formation of transient hydrophilic pores in the membrane occurred. It remained unclear if this was due to a rather small size of the patches considered in the simulations but in a more recent study, Koshiyama et al. (2010) have shown that such pores could form during the reorganization of a bilayer soaked with water. This effect was suggested as a possible mechanism of sonoporation, provided that shock waves lead to fast (subnanosecond) penetration of a huge quantity of water into the lipid hydrophobic region. However, it should be mentioned that their simulations did not consider the presence of gas microbubbles.

10.2.2 Hypothesized Impacts of Acoustic Phenomena on Cell Membrane and Molecular Uptake

The mechanisms involved in the sonoporation process and the cell membrane permeabilization remain poorly identified. Although no consensus

has been reached, several scenarios have been hypothesized, such as the formation of pores, further stimulation of endocytotic pathways and the occurrence of membrane wounds. Elucidating the mechanisms responsible for the delivery of compounds to cells and the kinetics of permeabilization is essential for improving and controlling this therapeutic strategy.

10.2.2.1 Pore Formation

One of the earliest reports on the formation of pores on the cell membrane after ultrasound insonation dates to (1999). The study showed that applying ultrasound at 255 kHz to a suspension of HL-69 cells in presence of photosensitive drug induced cell porosity where craters were observed on the cell membrane. The authors concluded that such holes or craters are responsible for cell killing.

In 2005, the group from Bracco reported the formation of small pores in the nanometer range on MAT B III cells (2005). Using dextran markers of various sizes as drug mimics, they concluded that molecules of a diameter ranging from 11 to 37 nm crossed the membrane and entered in the cell through the formation of small pores. The group from Gent University (Geers et al. 2011) studied the transduction of cells by means of adeno-associated-virus (AAV) as a vector, which totally relies on the receptor-mediated endocytosis to successfully transduce the cells using BLM melanoma cells. They made the use of pegylated AAV, which reduces strongly the endocytosis of AAV. The cells were then transduced using the BacMam™ 2.0 technique (GFP-reporter gene targeting the Rab5a). They observed no significant colocalization of these red-labeled vectors with the green-labeled endosomes, as no merged green and red (orange) signals could be observed inside the cells meaning that molecules ranging from 20 to 30 nm entered through pores only. These results are in contradiction with those reported earlier by the Dutch team (Meijering et al. 2009). By studying the cellular localization of fluorescent dextrans after sonoporation, they found that the smaller dextran molecules of 4.4 and 70 kDa were homogeneously distributed throughout the cytosol. This is similar to the

cellular distribution found after the microinjection of dextran molecules from 3 to 70 kDa (3–8 nm) into the cytosol indicating that during sonoporation, the small dextran molecules enter cells via transient pores in the cell membrane. In contrast, dextran molecules of 155 and 500 kDa (>17 nm) were mainly localized in vesicle-like structures after sonoporation, indicating that the larger dextrans might be taken up via endocytosis. When these dextran molecules had entered via pores, a homogeneous cytosolic distribution would be expected, comparable to the distribution of these dextran molecules after microinjection. They concluded that molecules of a size less than 17 nm entered through pores while molecules larger than 17 nm entered through endocytosis pathways. Nevertheless, they did not indicate which endocytosis pathways might be involved.

Zhou et al. (2012) used controlled manipulation techniques to correlate the ultrasound-generated bubble activities with the cell membrane poration using *Xenopus* oocyte. They attributed the change in membrane permeability to a sub-micrometer pore caused by a local membrane rupture formed by bubble collapse or bubble compression depending on ultrasound amplitude and duration. The study was extended to investigate the sonoporation and to quantify the size and the resealing rate of the pores on a single cell using cell-attached microbubbles (2012).

Recently, Hu et al. (2013) have shown by using a cell/microbubble ratio of 1:1 that a localized perforation of the cell membrane occurs immediately upon application of a 10-cycle ultrasound pulse. It was also demonstrated that the pore creation (5.3 μm long axis diameter) was synchronized with the time of bubble collapse. This membrane disruption is transient as membrane resealing commenced within 5 s after the incidence of sonoporation, and took between 6 and 20 s to be fully restored. In contrast, large pores (12–32.6 μm) appeared following sonoporation, but did not reseal.

10.2.2.2 Endocytosis

Endocytosis pathways have been hypothesized as a mechanism of a potential plausible route for

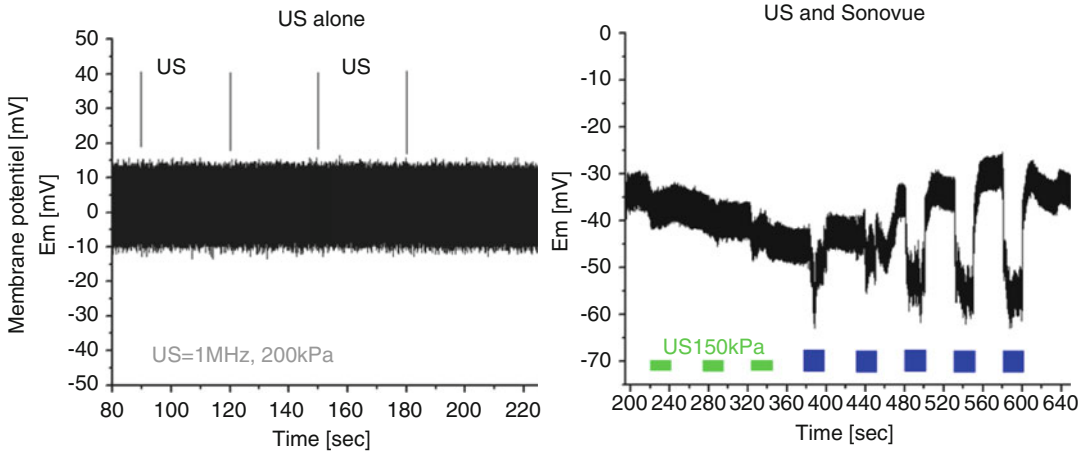


Fig. 10.3 Cell membrane potential after ultrasound insonation (*left*) and ultrasound and SonoVue microbubbles (*right*)

molecule incorporation into cells after sonoporation. A number of cellular reactions observed after ultrasound activation were attributed to molecular uptake, including ion exchange, hydrogen peroxide and cell intracellular calcium concentration.

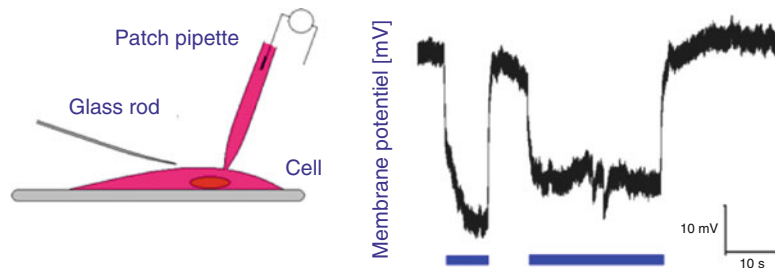
Fluorescence (Lionetti et al. 2009; Meijering et al. 2009; Paula et al. 2011) and electron microscopy (Saito et al. 1999; Mehier-Humbert et al. 2005; Duvshani-Eshet et al. 2006; Yang et al. 2008; Hauser et al. 2009) studies showed an exceedingly high amount of endocytic vesicles and clathrin coated pits in sonicated cells group, while control cell sections showed single endocytic vesicles. It is believed that Ca^{2+} controls the uncoating of clathrin-coated pits, thus high concentrations of calcium in the cytosol are thought to trigger the uncoating of endocytic vesicles. Therefore, calcium presumably plays a crucial role in the turnover of clathrin-coated vesicles (Hauser et al. 2009).

Tran et al. (2007) investigated the implication of endocytosis routes in the sonoporation mechanisms. Ruptured-patch clamp whole-cell technique was used to measure membrane potential variations of a single cell in the presence of SonoVue microbubbles after application of ultrasound waves at 1 MHz. Microbubbles and cells were simultaneously video monitored during ultrasound exposure. The results displayed in Fig. 10.3 showed that, during sonoporation, a

marked cell membrane hyperpolarization occurs at negative pressure amplitudes above 150 kPa, indicating the activation of specific ion channels, while the cell and the microbubbles remain viable. The hyperpolarization was sustained for as long as the microbubbles were in a direct contact with the cell and the ultrasound waves were transmitted. Smaller acoustic amplitudes induced only mild hyperpolarization, whereas shutting off the ultrasound brought the cell membrane potential to its resting value. However, ultrasound alone did not affect the cell membrane potential.

A similar hyperpolarization of the cell membrane was observed when mechanical pressure was applied to the cell through a glass probe (Fig. 10.4). The change in cell membrane potential indicates the activation of specific ion channels and depends on the quality of microbubble adhesion to the cell membrane. The use of IbTx showed that microbubbles induced a mechanical stretch activating BK_{Ca} channels. Simultaneous Ca^{2+} measurements indicate a slow and progressive Ca^{2+} increase, which is likely to be a consequence of BK_{Ca} channels opening but not a cause. In conclusion, these results demonstrate that microbubble oscillations under ultrasound activation entail the modulation of cellular function and signaling by triggering the modulation of ionic transports through the cell membrane. Cell response to the mechanical stretch caused by gentle microbubble oscillations is characterized

Fig. 10.4 Cell membrane potential after the application of manual mechanical pressure



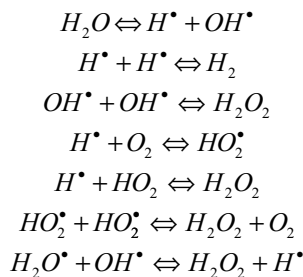
by the opening of BK_{Ca} stretch channels and a Ca^{2+} flux, which might potentially trigger other cellular reactions responsible for membrane sonopermeabilization.

Juffermans et al. (2006) have observed chemical stress by inducing the formation of free radicals. A significant increase in the production of H_2O_2 after ultrasound-exposed MBs compared with US alone, inducing Ca^{2+} influxes and thus cell membrane permeabilization. At physiological $[Ca^{2+}]_0$, ultrasound application caused immediate $[Ca^{2+}]_i$ transients in some cells, followed by delayed initiation of $[Ca^{2+}]_i$ transients in other surrounding cells (Kumon et al. 2009; Fan et al. 2010). The delay time can be up to 1 min or more. In addition, significant calcium transients and waves were distinctly correlated spatially and temporally with the application of ultrasound and only occurred in the presence of microbubbles. Furthermore, cell-to-cell contact is not always necessary for calcium waves to occur (Sauer et al. 2000).

Similar results have been reported by Juffermans et al. (2008), in which they demonstrated that US-exposed microbubbles caused an influx of calcium ions and local hyperpolarization of the cell membrane in rat cardiomyoblast cells. The same group reported in 2009 (Juffermans et al. 2009), using the same cells, the effect of oscillating microbubbles on a number of cellular parameters. They demonstrated increased membrane permeability for calcium ions, with an important role of hydrogen peroxide (H_2O_2). Further changes in ROS homeostasis involved an increase in intracellular H_2O_2 levels, protein nitrosylation and a decrease in total endogenous glutathione levels.

It has long been reported that during microbubble collapse, extremely high pressures on the

order of hundreds of atmospheres and extremely high temperatures on the order of thousands of degrees Kelvin are generated in the vapor phase inside the bubble. These processes were shown to produce under certain conditions highly reactive free radicals. The results of spin-trapping and electron spin resonance studies provided evidence for the formation of hydroxyl radicals OH^\bullet and hydrogen atoms H^\bullet during the sonolysis of aqueous solutions (Makino et al. 1982; Didenko and Suslick 2002). Sonochemistry reports in fact several primary reaction mechanisms that are believed to occur during sonication:



These reactions have been considered in sophisticated models to explain experimentally observed sonochemical phenomena (Didenko and Suslick 2002). Comparing three clinically used US contrast agents, Hassan et al. (2010) showed that both shell elasticity and reactivity played a role in modulating the extent of ultrasound-induced free-radical formation. The role of free radicals in the phenomenon of cell membrane permeabilization was also assessed using ultrasound alone (Lionetti et al. 2009). The authors showed that ultrasound at high intensities (mechanical index >1) was able to enhance endothelial caveolar internalization of recombinant EGFP fusion protein, while free-radical

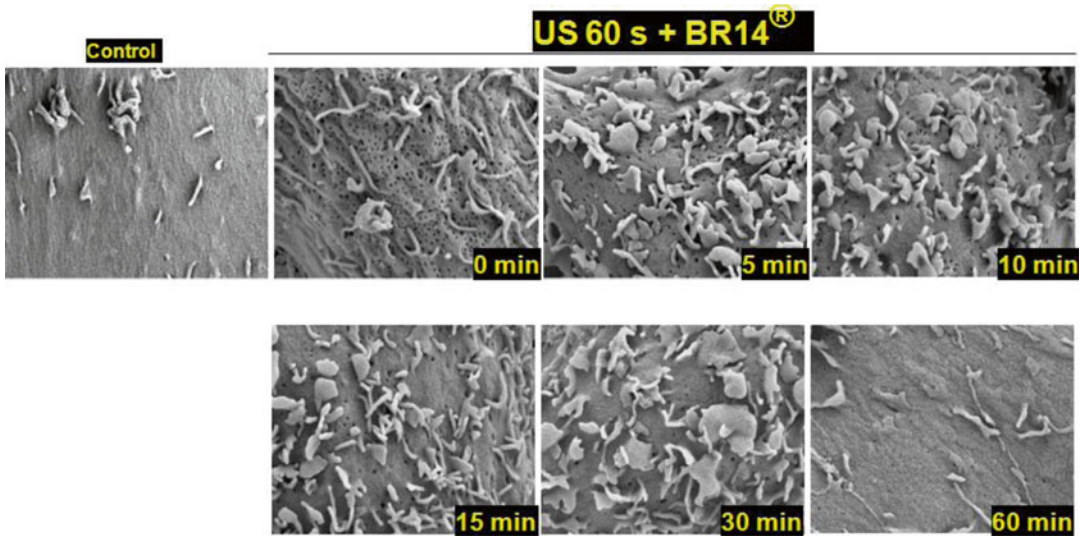


Fig. 10.5 SEM Observations of U-87 MG cells insonified with ultrasound in the presence of BR14 microbubbles. The cells were fixed immediately, and then at different time points after sonoporation

generation inhibitors, such as catalase and superoxide dismutase, reduced the induced internalization by a 49.29 % factor.

Taken together, these results indicate that sonoporation induces an activation of ionic channels, formation of hydrogen peroxide and influx of calcium ions. These cellular reactions are known to be directly related to endocytosis. More recently, the implication of caveole-endocytosis pathways in the mechanisms of cell membrane permeabilization using ultrasound and microbubbles has been hypothesized. In this study, scanning electron microscopy (SEM) was used to investigate the dynamic ultra-structural modifications of cell membranes, induced by sonoporation (Zeghimi et al. 2012). The study showed that sonoporation in the presence of microbubbles induced the formation of a significant number of permeant structures (TPS) at the membrane level. These structures were transient with a half-life of 15 min and had a heterogeneous size distribution ranging from a few nanometers to 150 nm (Fig. 10.5). The number and the size of these structures were positively correlated with the enhanced intracellular uptake of non-permeant molecules (Sytox Green).

Transmission electron microscopy (TEM) images showed a large number of uncoated pits at

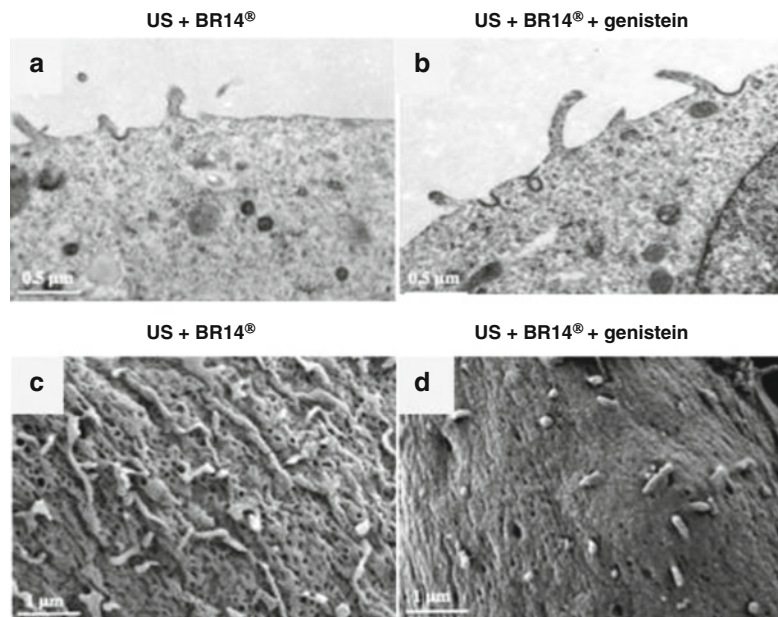
the plasma membrane level of the cells, which suggests that sonoporation probably increases the native permeability of plasma membranes through caveolae-dependent endocytosis pathways (Fig. 10.6a, b). This was confirmed when the cells were incubated with Genistein, a specific inhibitor of caveolae-endocytosis pathway. The number of uncoated pits for sonoporated cells pre-treated with genistein decreased significantly as compared to sonoporated cells without genistein incubation, thus suggesting that sonoporation stimulated the caveolae-dependent endocytosis.

10.2.2.3 Membrane Wounds

Tachibana et al. (1999) studied the structure of the cell surface with scanning electron microscopy after exposure to continuous wave ultrasound at low frequency (255 kHz). They showed that the cytoplasm of sonicated cells in the presence of a photosensitive drug appeared to get squeezed out through the cell surface, probably due to extensive cell membrane disruptions. These cells seemed to be non viable anymore.

Other studies using microscopic imaging and physical methods, such as shear forces, mechanically created wounds of sub-micrometer radius in the plasma membrane, through which

Fig. 10.6 Transmission electron microscopy images (a, b) and scanning electron microscopy images (c, d) of U-87 MG cells after sonoporation: (a, c) without genistein incubation; (b, d) with genistein incubation



molecules loading occurred (Fechheimer et al. 1987; Zarnitsyn et al. 2008). These wounds are resealed in time by the aggregation and the fusion of lipid vesicles trafficked to the wound site using an active cellular repair processes (McNeil and Terasaki 2001). Theoretical modeling predicted that membrane wounds would have a 300 nm radius initially, then they would shrink, with a half-life of 20–50 s, and then they are completely resealed in 900 s after sonication (Zarnitsyn et al. 2008). They assumed that (i) after the first second of cell wounding, the only mechanism governing the transport on the scale of seconds and minutes is passive diffusion through long-lived wounds in the plasma membrane, (ii) a “sufficiently large” number of nanopores are present in the wound, and (iii) the transport to and from the wound surface is rate-limiting; it is relatively fast because diffusion through the 5-nm-thick nanopores should be fast relative to diffusion between the bulk solution and the wound area.

Furthermore, Schlicher et al. (2010), using SEM, Cryo-SEM and LSCM (Laser Scanning Confocal Microscopy) on DU145 prostate-cancer cells, have reported that wounded cells produced spherically protruding “balloons” and “blister”

blebs which pinched off into the extracellular environment at the sites of plasma membrane disruption. The balloon blebs might contain small round lipid vesicles derived from endoplasmic reticulum, indicating that the blebs accessed the cytosol, while the “blister” blebs were created by lipids integrated with the plasma membrane and filled with clear fluid. Moreover, a loss or disruption of actin at sites of blebs formation was observed. In addition, this study reports that acoustic cavitation can also lead to multiple types of membrane blebbing, formation of perikarya, nuclear ejection and instant cell lysis, depending on the degree of wounding incurred.

Most of cells are able to resealed their membrane wounds, despite the damages of their plasma membrane (Andrew et al. 1999; Wu et al. 2002). The resealing of large wounds is similar to resealing processes to repair membrane patches damaged by micropipette insertion into a cell (McNeil and Steinhardt 2003). The repair of these wounds requires the recruitment of intracellular vesicles to the site of disruption and this process is ATP-dependent (Zarnitsyn et al. 2008). Also, it has been reported that the cell recovery after wounding might be related to bleb formation (Schlicher et al. 2010).

Conclusions

Sonoporation of cells and tissues by ultrasonically activated microbubbles is a fascinating phenomenon, which has intrigued many research laboratories worldwide in the last 15 years. More than 150 papers have been published on sonoporation *in-vitro*. Sonoporation was achieved using low frequency ultrasound (of the order of tens of kHz), shockwave lithotripters, medical therapeutic or even diagnostic ultrasound systems and various purpose built laboratory systems in the low MHz frequency range. The sonoporation activity can be generated by pre-existing cavitation nuclei, but better control of the process is achievable by adding stabilized microbubbles to the medium, such as ultrasound contrast agents.

The interaction of ultrasound and cells in the presence of contrast microbubbles induces a modulation of cell membrane permeability and as a result, molecules, which normally do not cross the barrier (cell membrane, endothelial layer), do penetrate into the cell. The transfer of these molecules seems to occur in association with various acoustic phenomena such as microstreaming, shear stress, shockwaves and microjets or a combination of them.

Despite a significant scientific progress during the last few years in the understanding of the cell-ultrasound and microbubble interaction, the mechanisms by which the molecules cross the biological barrier and enter into the cell cytoplasm after sonoporation are still not reasonably understood and no consensus is reached yet. Today, various hypotheses, including (i) non-selective poration of the cell membrane, (ii) endocytosis stimulation and (iii) formation of large cell membrane wounds, have been proposed. Moreover, there are various diverging reports on the duration of the permeabilization process after sonoporation. Some studies indicate transient permeabilization of a few seconds to minutes while other reports mention much longer permeabilization durations of up to 24 h.

A number of molecules have transferred into cells with sonoporation including Different molecules have been transferred into cells

using sonoporation, including small fluorescent molecules, RNA, plasmid DNA, plasmid lipoplexes, nanoparticles, anti-cancer drugs, anti-bodies and viruses. The types of sonoporation cells vary from primary cells in suspension or adherent configurations to bacteria and cancer cells. Sonoporation has been evaluated in various applications for gene and drug delivery and, as a result, many organs have been targeted with most of the applications directed to tumor, heart, brain and skeletal muscle.

In conclusion, although sonoporation has been extensively investigated with the aim of delivering therapeutic compounds and treating a number of pathologies, it is prudent to consider that the interaction of ultrasound and gaseous microbubbles with cells involves a degree of randomness and can sometimes engender lethal effects. It has been shown that sonoporation cells might undergo apoptosis, have poor cloning efficiency or can suffer from malfunction. Therefore, safety remains an important factor to be addressed before implementing the current results and the technology into the clinic.

References

- Andrew A, Brayman ML, Coppage S, Vaidya MWM (1999) Transient poration and cell surface receptor removal from human lymphocytes *in vitro* by 1 MHz ultrasound. *Ultrasound Med Biol* 25:999–1008
- Bao S, Thrall BD, Miller DL (1997) Transfection of a reporter plasmid into cultured cells by sonoporation *in vitro*. *Ultrasound Med Biol* 23:953–959
- Benjamin TB, Ellis AT (1966) The collapse of cavitation bubbles and the pressures thereby produced against solid boundaries. *Philos Trans R Soc A* 260:221–240
- Blake JR, Gibson DC (1987) Cavitation bubbles near boundaries. *Annu Rev Fluid Mech* 19:99–123
- Bloch SH, Dayton PA, Ferrara KW (2004) Targeted imaging using ultrasound contrast agents: progress and opportunities for clinical and research applications. *IEEE Eng Med Biol Mag* 23:18–29
- Brennen CE (1995) *Cavitation and bubble dynamics*. Oxford University Press, Oxford, pp 79–111
- Brujan EA, Nahen K, Schmidt P, Vogel A (2001a) Dynamics of laser-induced cavitation bubbles near an elastic boundary. *J Fluid Mech* 433:251–281
- Brujan EA, Nahen K, Schmidt P, Vogel A (2001b) Dynamics of laser-induced cavitation bubbles near

- elastic boundaries: influence of the elastic modulus. *J Fluid Mech* 433:283–314
- Brunton JH (1967) Erosion by liquid shock. In: Fyall AA, King RB (eds) *Proceedings of the 2nd international conference on rain erosion and allied phenomena*. Royal Aircraft Establishment, Farnborough, pp 291–309
- Collis J, Manasseh R, Liovic P, Tho P, Ooi A, Petkovic-Duran K, Zhu Y (2010) Cavitation microstreaming and stress fields created by microbubbles. *Ultrasonics* 50:273–279
- Davidson BJ, Riley N (1971) Cavitation microstreaming. *J Sound Vib* 15:217–233
- Didenko Y, Suslick KS (2002) The energy efficiency of formation of photons, radicals, and ions during single bubble cavitation. *Nature* 418:394–397
- Doinikov AA, Bouakaz A (2010a) Acoustic microstreaming around a gas bubble. *J Acoust Soc Am* 127:703–709
- Doinikov AA, Bouakaz A (2010b) Acoustic microstreaming around an encapsulated particle. *J Acoust Soc Am* 127:1218–1227
- Doinikov AA, Bouakaz A (2010c) Theoretical investigation of shear stress generated by a contrast microbubble on the cell membrane as a mechanism for sonoporation. *J Acoust Soc Am* 128:11–19
- Duvshani-Eshet M, Baruch L, Kesselman E, Shimoni E, Machluf M (2006) Therapeutic ultrasound-mediated DNA to cell and nucleus: bioeffects revealed by confocal and atomic force microscopy. *Gene Ther* 13:163–172
- Elder SA (1959) Cavitation microstreaming. *J Acoust Soc Am* 31:54–64
- Esoffre JM, Zeghimi A, Novell A, Bouakaz A (2013) In-vivo gene delivery by sonoporation: recent progress and prospects. *Curr Gene Ther* 13:2–14
- Fan Z, Kumon R, Park J, Deng CX (2010) Intracellular delivery and calcium transients generated in sonoporation facilitated by microbubbles. *J Control Release* 142:31–39
- Fechheimer M, Boylan JF, Parker S, Sisken JE, Patel GL, Zimmer SG (1987) Transfection of mammalian cells with plasmid DNA by scrape loading and sonication loading. *Proc Natl Acad Sci U S A* 84:8463–8467
- Ferrara K, Pollard R, Borden M (2007) Ultrasound microbubble contrast agents: Fundamentals and application to gene and drug delivery. *Annu Rev Biomed Eng* 9:415–447
- Field JE (1991) The physics of liquid impact, shock wave interactions with cavities, and the implications to shock-wave lithotripsy. *Phys Med Biol* 36:1475–1484
- Gac SL, Zwaan E, van den Berg A, Ohl CD (2007) Sonoporation of suspension cells with a single cavitation bubble in a microfluidic confinement. *Lab Chip* 7:1666–1672
- Geers B, Lentacker I, Alonso A, Sanders NN, Demeester J, Meairs S, De Smedt SC (2011) Elucidating the mechanisms behind sonoporation with adeno-associated virus-loaded microbubbles. *Mol Pharm* 8:2244–2251
- Goldberg BB, Raichlen JS, Forsberg F (2001) *Ultrasound contrast agents: basic principles and clinical applications*. Martin Dunitz, London
- Hassan MA, Feril LB Jr, Kudo N, Tachibana K, Kondo T, Riesz P (2010) The sonochemical and biological effects of three clinically-used contrast agents. *Jpn J Appl Phys* 49:1347
- Hauser J, Ellisman M, Steinau HU, Stefan Dudda M, Hauser M (2009) Ultrasound enhanced endocytotic activity of human fibroblasts. *Ultrasound Med Biol* 35:2084–2092
- Hughes DE, Nyborg WL (1962) Cell disruption by ultrasound. *Science* 138:108–114
- Hu Y, Wan JM, Yu AC (2013) Membrane perforation and recovery dynamics in microbubble-mediated sonoporation. *Ultrasound Med Biol* 39:2393–2405
- Juffermans LJM, van Dijk A, Jongenelen CA, Drukarch B, Reijerkerk A, de Vries HE, Kamp O, Musters RJ (2009) Ultrasound and microbubble-induced intra- and intercellular bioeffects in primary endothelial cells. *Ultrasound Med Biol* 35:1917–1927
- Juffermans LJM, Dijkmans PA, Musters RJP, Visser CA, Kamp O (2006) Transient permeabilization of cell membranes by ultrasound-exposed microbubbles is related to formation of hydrogen peroxide. *Am J Physiol Heart Circ Physiol* 291:H1595–H1601
- Juffermans LJM, Kamp O, Dijkmans PA, Visser CA, Musters RJ (2008) Low-intensity ultrasound-exposed microbubbles provoke local hyperpolarization of the cell membrane via activation of BK(Ca) channels. *Ultrasound Med Biol* 34:502–598
- Kaddur K, Palanchon P, Tranquart F, Pichon C, Bouakaz A (2007) Sonopermeabilization: Therapeutic alternative with ultrasound and microbubbles. *J Radiol* 88:1777–1786
- Klibanov AL (2006) Microbubble contrast agents: Targeted ultrasound imaging and ultrasound-assisted drug-delivery applications. *Invest Radiol* 41:354–362
- Kolb J, Nyborg W (1956) Small-scale acoustic streaming in liquids. *J Acoust Soc Am* 28:1237–1242
- Kornfeld M, Suvorov L (1944) On the destructive action of cavitation. *J Appl Phys* 15:495–506
- Koshiyama K, Kodama T, Yano T, Fujikawa S (2006) Structural change in lipid bilayers and water penetration induced by shock waves: molecular dynamics simulations. *Biophys J* 91:2198–2205
- Koshiyama K, Kodama T, Yano T, Fujikawa S (2008) Molecular dynamics simulation of structural changes of lipid bilayers induced by shock waves: effects of incident angles. *Biochim Biophys Acta* 1778:1423–1428
- Koshiyama K, Yano T, Kodama T (2010) Self-organization of a stable pore structure in a phospholipid bilayer. *Phys Rev Lett* 105:018105
- Krasovitski B, Kimmel E (2004) Shear stress induced by a gas bubble pulsating in an ultrasonic field near a wall. *IEEE Trans Ultrason Ferroelectr Freq Control* 51:973–979
- Kudo N, Okada K, Yamamoto K (2009) Sonoporation by single-shot pulsed ultrasound with microbubbles adjacent to cells. *Biophys J* 96:4866–4876
- Kumon RE, Aehle M, Sabens D, Parikh P, Han YW, Kourennyi D, Deng CX (2009) Spatiotemporal effects of sonoporation measured by real-time calcium imaging. *Ultrasound Med Biol* 35:494–506

- Lauterborn W (1972) High-speed photography of laser-induced breakdown in liquids. *Appl Phys Lett* 21:27–29
- Lauterborn W, Bolle H (1972) Experimental investigations of cavitation-bubble collapse in the neighbourhood of a solid boundary. *J Fluid Mech* 72:391–399
- Lauterborn W, Kurz T (2010) Physics of bubble oscillations. *Rep Prog Phys* 73:106501
- Leighton TG (1994) *The acoustic bubble*. Academic, London, pp 531–550
- Lewin PA, Bjørnø L (1982) Acoustically induced shear stresses in the vicinity of microbubbles in tissue. *J Acoust Soc Am* 71:728–734
- Lindau O, Lauterborn W (2003) Cinematographic observation of the collapse and rebound of a laser-produced cavitation bubble near a wall. *J Fluid Mech* 479:327–348
- Lionetti V, Fittipaldi A, Agostini S, Giacca M, Rechhia FA, Picano E (2009) Enhanced caveolae-mediated endocytosis by diagnostic ultrasound in vitro. *Ultrasound Med Biol* 35:136–143
- Liu RH, Yang J, Pindera MZ, Athavale M, Grodzinski P (2002) Bubble-induced acoustic micromixing. *Lab Chip* 2:151–157
- Liu X, Wu J (2009) Acoustic microstreaming around an isolated encapsulated microbubble. *J Acoust Soc Am* 125:1319–1330
- Longuet-Higgins MS (1998) Viscous streaming from an oscillating spherical bubble. *Proc R Soc Lond A* 454:725–742
- Makino K, Mossoba MM, Riesz P (1982) Chemical effects of ultrasound on aqueous solutions. Evidence for hydroxyl and hydrogen free radicals (.cntdot.OH and.cntdot.H) by spin trapping. *J Am Chem Soc* 104:3537–3539
- Maksimov AO (2007) Viscous streaming from surface waves on the wall of acoustically-driven gas bubbles. *Eur J Mech B Fluids* 26:28–42
- McNeil PL, Steinhardt RA (2003) Plasma membrane disruption: repair, prevention, adaptation. *Annu Rev Cell Dev Biol* 19:697–731
- McNeil PL, Terasaki M (2001) Coping with the inevitable: how cells repair a torn surface membrane. *Nat Cell Biol* 3:E124–E129
- Mehier-Humbert S, Bettinger T, Yan F, Guy RH (2005) Plasma membrane poration induced by ultrasound exposure: implication for drug delivery. *J Control Release* 104:213–222
- Meijering BDM, Juffermans LJM, van Wamel A et al (2009) Ultrasound and microbubble-targeted delivery of macromolecules is regulated by induction of endocytosis and pore formation. *Circ Res* 104:679–687
- Mørch KA (1979) Dynamics of cavitation bubbles and cavitation liquids. In: Preece CM (ed) *Erosion*. Academic, London, pp 309–353
- Naudé CF, Ellis AT (1961) On the mechanism of cavitation damage by nonhemispherical cavities collapsing in contact with a solid boundary. *Trans ASME D: J Basic Eng* 83:648–656
- Novell A, Collis J, Doinikov A, Ooi A, Manasseh R, Bouakaz A (2011) Theoretical and experimental evaluation of microstreaming created by a single microbubble: application to sonoporation. *Book Series: IEEE International Ultrasonics Symposium, Orlando, USA* pp 482–485
- Nyborg WL (1958) Acoustic streaming near a boundary. *J Acoust Soc Am* 30:329–339
- Nyborg WL (1978) Physical principles of ultrasound. In: Fry FJ (ed) *Ultrasound: its applications in medicine and biology, Part I*. Elsevier, New York, USA pp 1–75
- Ohl CD, Arora M, Ikink R, de Jong N, Versluis M, Delius M, Lohse D (2006) Sonoporation from jetting cavitation bubbles. *Biophys J* 91:4285–4295
- Ohl CD, Kurz T, Geisler R, Lindau O, Lauterborn W (1999) Bubble dynamics, shock waves and sonoluminescence. *Phil Trans R Soc Lond A* 357:269–294
- Paula DMB, Valero-Lapchik VB, Paredes-Gamero EJ, Han SW (2011) Therapeutic ultrasound promotes plasmid DNA uptake by clathrin-mediated endocytosis. *J Gene Med* 13:392–401
- Plesset MS, Prosperetti A (1977) Bubble dynamics and cavitation. *Annu Rev Fluid Mech* 9:145–185
- Pritchard NJ, Hughes DE, Peacocke AR (1966) The ultrasonic degradation of biological macromolecules under conditions of stable cavitation. I. Theory, methods and application to deoxyribonucleic acid. *Biopolymers* 4:259–273
- Rooney JA (1970) Hemolysis near an ultrasonically pulsating gas bubble. *Science* 169:869–871
- Rooney JA (1972) Shear as a mechanism for sonically induced biological effects. *J Acoust Soc Am* 52:1718–1724
- Ross JP, Cai X, Chiu JF, Yang J, Wu J (2002) Optical and atomic force microscopic studies on sonoporation. *J Acoust Soc Am* 111:1161–1164
- Saito K, Miyake K, McNeil PL, Kato K, Yago K, Sugai N (1999) Plasma membrane disruption underlies injury of the corneal endothelium by ultrasound. *Exp Eye Res* 68:431–437
- Sauer H, Hescheler J, Wartenberg M (2000) Mechanical strain-induced Ca²⁺ waves are propagated via ATP release and purinergic receptor activation. *Am J Physiol Cell Physiol* 279:C295–C307
- Schlicher RK, Hutcheson JD, Radhakrishna H, Apakarian RP, Prausnitz MR (2010) Changes in cell morphology due to plasma membrane wounding by acoustic cavitation. *Ultrasound Med Biol* 36:677–692
- Shima A, Takayama K, Tomita Y, Ohsawa N (1983) Mechanism of impact pressure generation from spark-generated bubble collapse near a wall. *AIAA J* 21:55–59
- Szabo T (2004) *Diagnostic ultrasound imaging: inside out*. Academic, New York
- Tachibana K, Uchida T, Ogawa K, Yamashita N, Tamura K (1999) Induction of cell-membrane porosity by ultrasound. *Lancet* 353:1409
- Tho P, Manasseh R, Ooi A (2007) Cavitation microstreaming in single and multiple bubble systems. *J Fluid Mech* 576:191–233
- Tran TA, Roger S, Le Guennec JY, Tranquart F, Bouakaz A (2007) Effect of ultrasound-activated microbubbles on the cell electrophysiological properties. *Ultrasound Med Biol* 33:158–163

- van Wamel A, Bouakaz A, Versluis M, de Jong N (2004) Micromanipulation of endothelial cells: ultrasound-microbubbles-cell interaction. *Ultrasound Med Biol* 30:1255–1258
- Vogel A, Lauterborn W, Timm R (1989) Optical and acoustic investigations of the dynamics of laser-produced cavitation bubbles near a solid boundary. *J Fluid Mech* 206:299–338
- Vyas B, Preece CM (1976) Stress produced in a solid by cavitation. *J Appl Phys* 47:5133–5138
- Wang C, Jalikop SV, Hilgenfeldt S (2012) Efficient manipulation of microparticles in bubble streaming flows. *Biomicrofluidics* 6:012801
- Wu J (2002) Theoretical study on shear stress generated by microstreaming surrounding contrast agents attached to living cells. *Ultrasound Med Biol* 28:125–129
- Wu J, Du G (1997) Streaming generated by a bubble in an ultrasound field. *J Acoust Soc Am* 101:1899–1907
- Wu J, Nyborg WL (2008) Ultrasound, cavitation bubbles and their interaction with cells. *Adv Drug Deliv Rev* 60:1103–1116
- Wu J, Ross JP, Chiu JF (2002) Repairable sonoporation generated by microstreaming. *J Acoust Soc Am* 111:1460
- Yang F, Gu N, Chen D, Xi X, Zhang D, Li Y, Wu J (2008) Experimental study on cell self-sealing during sonoporation. *J Control Release* 131:205–210
- Yu H, Chen S (2014) A model to calculate microstreaming-shear stress generated by oscillating microbubbles on the cell membrane in sonoporation. *Biomed Mater Eng* 24:861–868
- Zarnitsyn V, Rostad CA, Prausnitz MR (2008) Modeling transmembrane transport through cell membrane wounds created by acoustic cavitation. *Biophys J* 95:4124–4138
- Zeghimi A, Uzbekov R, Escoffre JM, Arbeille B, Bouakaz (2012) Ultrastructural modifications of cell membranes and organelles induced by sonoporation. Book Series: IEEE International Ultrasonics Symposium, Dresden, Germany pp 2045–2048
- Zhou Y, Yang K, Cui J, Ye JY, Deng CX (2012) Controlled permeation of cell membrane by single bubble acoustic cavitation. *J Control Release* 157:103–111